Anomalous Electronic Structure and Pseudogap Effects in $Nd_{1.85}Ce_{0.15}CuO_4$

N. P. Armitage, D. H. Lu, C. Kim, A. Damascelli, K. M. Shen, F. Ronning,
D. L. Feng, P. Bogdanov, and Z.-X. Shen
Department of Physics, Applied Physics and Stanford Synchrotron Radiation Laboratory, Stanford University, Stanford, California 94305

Y. Onose, Y. Taguchi, and Y. Tokura
Department of Applied Physics, The University of Tokyo, Tokyo 113-8656, Japan

P. K. Mang, N. Kaneko, and M. Greven
Department of Applied Physics and Stanford Synchrotron Radiation Laboratory, Stanford University, Stanford, California 94305

(Received 21 December 2000; revised manuscript received 7 May 2001; published 18 September 2001)

We report a high-resolution angle-resolved photoemission spectroscopic study of the electron-doped (n-type) cuprate superconductor $Nd_{1.85}Ce_{0.15}CuO_4$. We observe regions along the Fermi surface where the near-E_F intensity is suppressed and the spectral features are broad in a manner reminiscent of the high-energy "pseudogap" in the underdoped p-type (hole doped) cuprates. However, instead of occurring near the $(\pi, 0)$ region, as in the p-type materials, this pseudogap falls near the intersection of the underlying Fermi surface with the antiferromagnetic Brillouin zone boundary.

DOI: 10.1103/PhysRevLett.87.147003 PACS numbers: 74.25.Jb, 74.72.Jt, 79.60.Bm

The electron-doped cuprate superconductors provide a unique opportunity to study the physics of doped Mott insulators and high-T_c superconductors. In addition to possessing interesting physics in their own right, the n-type materials, with their different normal state properties and phase diagram, offer an alternative venue to test various theories of high-T_c superconductivity.

$Nd_{2-x}Ce_xCuO_{4\pm\delta}$ is a member of the small family of cuprate superconductors that can be doped with electrons [1]. Only an approximate symmetry in the phase diagram exists about the zero doping line between the p-type and the n-type, as the antiferromagnetic phase is much more robust in the electron-doped material and persists to much higher doping levels. Superconductivity occurs in a doping range that is almost 5 times narrower. In addition, these two ground states occur in much closer proximity to each other. Experiments show additional contrasting behavior between n-type superconductors and their p-type counterparts [2].

Here we report a detailed angle-resolved photoemission spectroscopic (ARPES) study of the electronic structure of this electron-doped cuprate superconductor. Significant differences are found between it and the p-type materials that shed light on a number of important topics in the high-T_c superconductors. We find that the Luttinger volumed Fermi surface is truncated into several pieces with a high-energy "pseudogap"-like suppression that forms not at the maximum of the d-wave functional form as in the underdoped p-type materials, but near the intersections of the Fermi surface with the antiferromagnetic Brillouin zone (AFBZ) boundary.

Single crystals of $Nd_{1.85}Ce_{0.15}CuO_4$ (NCCO) were grown by the traveling-solvent floating-zone method in 4 atm of O_2. Details of this growth can be found elsewhere [3]. The resulting crystals show an onset of superconductivity at 25 K and a superconducting volume (Meissner shielding) of almost 100% at 20 K. A second batch of crystals, grown at Stanford University under similar conditions, showed an onset at 24 K with similarly narrow transition widths. The photoemission data obtained with the two batches are identical.

As it is imperative to determine which characteristics of the data are intrinsic and which are possible artifacts due to, for instance, the matrix elements for photoexcitation, data were collected on two different photoemission systems. On beam line 5-4 at the Stanford Synchrotron Radiation Laboratory (SSRL), data were taken at 16.5 eV photon energy ($\hbar\omega$) with an incident angle of approximately 45° and the in-plane polarization along the Cu-O bonds (energy resolution $\Delta E \simeq 10$ meV and angular resolution $\Delta\theta \simeq 0.5°$). At beam line 10.0.1 at the Advanced Light Source an incident energy of 55 eV was used in a glancing incidence geometry with in-plane polarization at 45° to the Cu-O bonds ($\Delta E \simeq 20$ meV, $\Delta\theta \simeq 0.25°$). All displayed spectra were taken at low temperature (10−20 K) in the superconducting state; this does not change the conclusions we make regarding the normal state electronic structure as the changes in the spectra with the onset of superconductivity are very subtle in NCCO [4]. The chamber pressure was lower than 4×10^{-11} torr. Cleaving the samples at low temperature *in situ* results in shiny flat surfaces which low-energy electron diffraction (LEED) [Fig. 2(c), below] reveal to be clean and well ordered, with a symmetry commensurate with the bulk. No signs of surface aging were seen for the duration of the experiment (~24 hours).

In Figs. 1(a)–1(c), we display energy distribution curves (EDCs) from high symmetry lines in the Brillouin zone (BZ) taken on the SSRL apparatus. In Fig. 1(a), one sees a dispersion along the Γ to (π,π) direction which is ubiquitous among the cuprates. A broad feature disperses quickly towards the Fermi energy (E_F), sharpens to a sharp peak at $\vec{k}_F$ $(0.46\pi, 0.46\pi)$, and then disappears. Along the Γ to $(\pi,0)$ direction, the n-type spectra are quite different from their p-type counterparts. While the low-energy feature in the optimally doped p-type compounds disperses quite close to E_F and forms a flat band region with a correspondingly high density of states close to E_F, in NCCO this flat band region is at about 300 meV higher energy [5]. Along $(\pi,0)$ to (π,π) [Fig. 1(c)], the peak disperses to E_F and gives a small peak at $\vec{k}_F$. The spectra also possess a large background contribution that has a weak maximum at 300 meV, as seen in the 100% curves in Figs. 1(a) and 1(c).

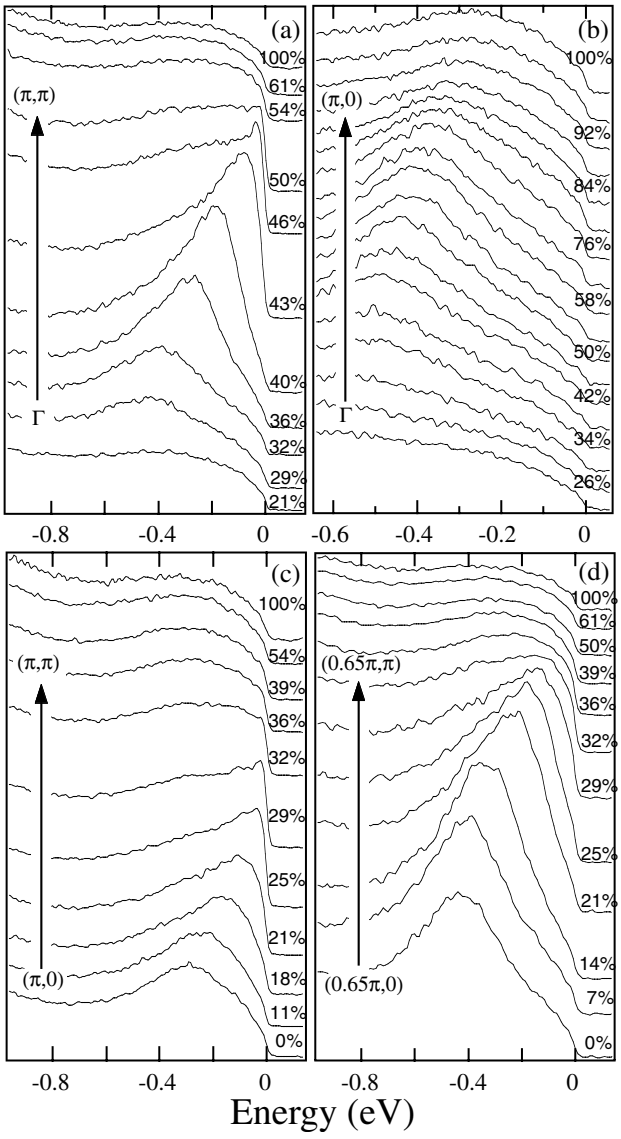

FIG. 1. Energy distribution curves from various directions in the Brillouin zone taken with $\hbar\omega = 16.5$ eV at SSRL. (a) $\Gamma-(\pi,\pi)$, (b) $\Gamma-(\pi,0)$, (c) $(\pi,0)-(\pi,\pi)$, (d) $(0.65\pi,0)-(0.65\pi,\pi)$. For a schematic refer to the black arrows in Fig. 2(a).

In addition to the spectra from the high-symmetry directions, more comprehensive intensity maps were obtained over a large region in momentum space at both photon energies. In Figs. 2(a) and 2(b), we have plotted the integrated spectral weight of the EDCs ($\hbar\omega = 16.5$ and 55 eV, respectively), from within a 30 meV window about E_F, as a function of $\vec{k}$. This gives a measure of the regions in momentum space that dominate the low-energy properties of the material, i.e., the Fermi surface. The expected large Fermi surface [as depicted in Fig. 2(d)] has a volume greater than $1/2$ (measured filling level $\delta = 1.12 \pm 0.05$) and has a shape that is consistent with the LDA band calculations [7]. Interestingly however, it shows two regions of suppressed spectral weight near $(0.65\pi, 0.3\pi)$ and $(0.3\pi, 0.65\pi)$. Although there is obviously some modulation of the intensity due to matrix elements, as some of the details of the intensity pattern are different between the two excitation energies, the gross features are the same. In addition, data from SSRL at 16.5 eV with the sample turned so that the polarization is at 45° to the Cu-O bond reveals a similar pattern (not shown). The fact that the same systematics are seen in different configurations gives us confidence that we are measuring intrinsic properties, a

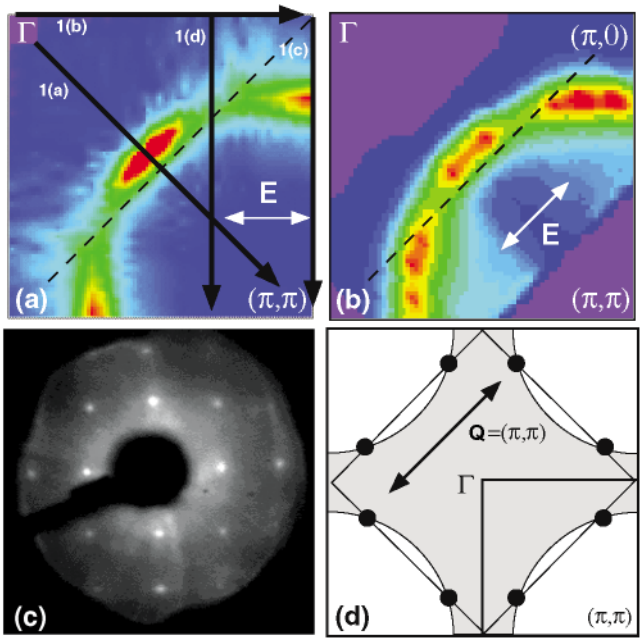

FIG. 2 (color). (a),(b) Fermi surface of the partial Brillouin zone of NCCO taken with $\hbar\omega = 16.5$ and 55 eV, respectively. The plotted quantity is a 30 meV integration about E_F of each EDC plotted as a function of $\vec{k}$. 16.5 eV data were taken over a Brillouin zone octant and symmetrized across the Γ to the (π,π) line, while the 55 eV data were taken over a full quadrant [6]. The polarization direction is denoted by the double ended arrow. The dotted line is the antiferromagnetic Brillouin zone boundary. (c) LEED spectra of NCCO cleaved *in situ* at 10 K. (d) Schematic showing only those regions of FS near the black circles can be coupled with a (π,π) scattering.

fact which will be substantiated by line shape analysis below.

A detailed look at $\hbar\omega = 16.5$ eV EDCs through the suppressed region of the Fermi surface [Fig. 1(d)] reveals that the peak initially approaches E_F and then monotonically loses weight despite the fact that its maximum never comes closer than $\sim$100 meV to E_F. Such behavior with broad features and suppression of low-energy spectral weight is similar to the high-energy pseudogap seen in the extreme underdoped p-type materials, although in the present case it is observed near $(0.65\pi, 0.3\pi)$ and not at $(\pi, 0)$, the maximum of the d-wave functional form. An additional important difference is that a true clean gap at the very lowest energies cannot be defined, because the continually decreasing slope of the EDCs at $\vec{k}_F$ gives a leading edge midpoint that is within a few meVs of E_F. We need to make the distinction between such high-energy pseudogap behavior and low-energy pseudogap behavior which is the clean leading edge gap seen in the normal state of underdoped and optimally doped p-types near $(\pi, 0)$ that has been posited to reflect pairing fluctuations in the normal state. The fact that they share the same d-wave functional form in the p-types has led to proposals that the pairing in the superconductor is an inherited property of the insulating state [8].

In Figs. 3(a) and 3(c), we plot $\hbar\omega = 55$ and 16.5 eV EDCs from around $\vec{k}_F$ from $(\pi/2, \pi/2)$ to $(\pi, 0.3\pi)$ as shown in the inset. Consistent with the intensity maps in Figs. 2(a) and 2(b), the data show a well-defined and intense peak at E_F in momentum space regions close to the

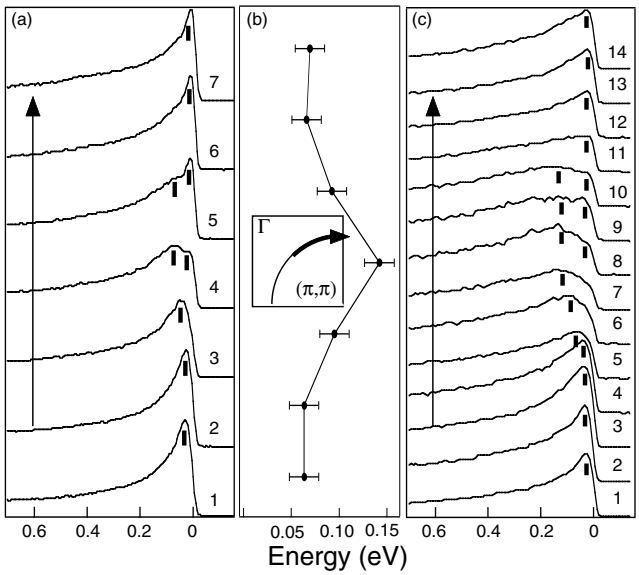

FIG. 3. (a) EDCs from along the $\vec{k}_F$ contour for $\hbar\omega = 55$ eV. The graph plots $(\pi/2, \pi/2)$ on the bottom and goes to $(\pi, 0.3\pi)$ at the top along the $\vec{k}_F$ contour given in the inset. (b) ΔE (defined as FWHM/2) for EDCs in (a). (c) $\hbar\omega = 16.5$ EDCs along the same $\vec{k}_F$ contour. The large momentum independent background [defined as the signal at (π, π)] has been subtracted out.

Γ to (π, π) Fermi surface crossing and to the $(\pi, 0)$ to (π, π) Fermi surface crossing. In between these regions, the spectra are rather different with no well-defined peaks. These line shapes prove that the major effects seen in the intensity plots are not due to matrix elements, which will not change the shape of the spectra drastically. These assertions receive further support from the measurement of EDC widths in Fig. 3(b). Here we plot the width in energy of the EDCs (defined as the FWHM/2 of the actual features and not the output of a fit) in Fig. 3(a). This quantity, which can be viewed as an average over the low-energy scattering rate ($\mathrm{Im}\Sigma$) is largest in the momentum region of interest along k_F where the near-E_F spectral weight is suppressed maximally as shown in Figs. 2(a) and 2(b). This analysis reveals that those regions along the FS that show the anomalous low-energy spectral weight suppression are subject to the strongest scattering effects.

We take the view that this anomalous electronic structure in the suppressed region reflects the transfer of spectral weight from a near-E_F peak to a large broader incoherent maximum at higher energy. As one moves along the Fermi surface from $(\pi/2, \pi/2)$ to $(\pi, 0.3\pi)$, this high-energy part at first gains intensity and shifts the global maxima to higher energy. In the intermediate region along the $\vec{k}_F$ contour, the near-E_F weight is suppressed maximally with most spectral weight at higher energy. Moving towards $(\pi, 0.3\pi)$, the high-energy part still forms a maximum at $\sim$100 meV but the low-energy peak begins to recover at E_F and the two features can be seen simultaneously in a single spectrum. The low-energy peak continues to gain weight until the zone edge at $\sim(\pi, 0.3\pi)$, while the high-energy part loses intensity and disappears. The point of view that the two features are part of a single spectral function is supported by the fact that we observe only a single Fermi surface with the expected Luttinger volume.

We note that the regions of momentum space with the unusual low-energy behavior fall intriguingly close to the intersection of the underlying FS with the AFBZ boundary, as shown by the dashed lines in Figs. 2(a) and 2(b). This suppression of low-energy spectral weight and the large scattering rate in certain regions on the FS resembles various theoretical predictions that emphasize a coupling of charge carriers to a low-energy collective mode with typical momentum (π, π). A simple phase space argument such as that shown in Fig. 2(d) shows that those charge carriers which lie at the intersection of the FS with the AFBZ boundary will suffer the largest effect of anomalous (π, π) scattering as these are the only FS locations that can have low-energy coupling with $\vec{Q} = (\pi, \pi)$. This low-energy scattering channel does not need to be antiferromagnetic for this role played by the AFBZ boundary to hold, only that its characteristic wave vector only needs to be (π, π). These heavily scattered regions of the FS have been referred to in the literature as "hot spots." It has been suggested that the large backscattering felt by charge carriers in the hot spots is the origin of the pseudogap in the underdoped hole-type materials [9].

A few candidates for such a scattering channel have been proposed. One realization would be a strong coupling of the charge carriers to (π, π) magnetic fluctuations. Strong AF fluctuations have been found at (π, π), as may have been expected in a material that is as close to the antiferromagnetic phase as this one [10]. In this context the pseudogap is seen as a precursor to the formation of the antiferromagnetic phase. Other possibilities include coupling to short range fluctuations of the charge density wave, d-density wave, or phononic type. A great deal of theoretical effort has been devoted to schemes based on the above general considerations [9,11,12]. Of course, we cannot rule out a combination of effects. Alternatively, large effective (π, π) scattering can be caused by umklapp (U) processes which are allowed only for charge carriers on the AFBZ boundary [13].

In the underdoped p-type materials, due to band filling considerations, the underlying Fermi surface area is smaller and, hence, its intersection with the AFBZ boundary is closer to $(\pi, 0)$. This, along with the existence of the near-E_F $(\pi, 0)$ extended saddle points, would cause these regions of the Brillouin zone to feel the largest effect of (π, π) couplings if such processes exist. As alluded to earlier, this may lead to the formation of a pseudogap whose momentum dependence closely mimics, and can be confused with, the functional form of the d-wave superconducting gap. In the present case of NCCO, the underlying Fermi surface is more distant from the $(\pi, 0)$ regions and the band there is flat 300 meV below E_F. In this scenario, the pseudogap regions would move away from $(\pi, 0)$ on the FS and along $\vec{k}_F$ towards $(\pi/2, \pi/2)$, as observed.

The class of theories that predict pseudogap formation at the intersection of the AFBZ boundary with the FS contrast with those that explain high-energy pseudogap and hot spot effects to result from fluctuations of a very large energy superconducting pairing scale that has been inherited from the AF insulator. The latter class of theories predicts that the momentum dependence of the pseudogap will follow the general trend of the d-wave superconducting gap, i.e., attaining a maximum value at $(\pi, 0)$. In the very underdoped regime in the p-type materials, ARPES measures a high-energy d-wave-like pseudogap on the order of 100 meV near the $(\pi, 0)$ region [14]. As we observe a high-energy pseudogap in NCCO of a similar energy scale, but with a very different momentum dependence, our results demonstrate the possibility that this very large d-wave-like pseudogap in the extreme underdoped p-type materials may not be related to preformed pairs, but instead may be due to preemergent magnetic order or other similar phenomena. Our observation still allows for the existence of a normal state low-energy pseudogap (defined by the leading edge) that may be related to the existence of pairing fluctuations above T_c. In this regard it appears that one must carefully discriminate between high-energy pseudogap behavior, which may be caused by the effects discussed above and is tied to the intersection of the FS with the AFBZ boundary, and pairing fluctuations that may cause pseudogap behavior on a lower energy scale and should follow the d-wave functional form. If one wishes to interpret the physics of the p- and n-type cuprates in a comprehensive fashion, then our results suggest that some of the confusing pseudogap phenomenology regarding energy scales and doping dependencies may be reconciled by distinguishing effects of these kinds.

We thank X. J. Zhou and Z. Hussain for beam line support. The Stanford Synchrotron Radiation Laboratory and the Advanced Light Source are both operated by the DOE Office of Basic Energy Science, Division of Chemical Sciences and Material Sciences. Additional support comes from the Office of Naval Research: ONR Grants No. N00014-95-1-0760/N00014-98-1-0195. The Tokyo crystal growth work was supported in part by Grants-in-Aid for Scientific Research from the Ministry of Education, Science, Sports, and Culture, Japan, and the New Energy and Industrial Technology Development Organization of Japan (NEDO). The crystal growth at Stanford was supported by the U.S. Department of Energy under Contracts No. DE-FG03-99ER45773 and No. DE-AC03-76SF00515, by NSF CAREER Award No. DMR-9985067, and by the A. P. Sloan Foundation.

[1] Y. Tokura, H. Takagi, and S. Uchida, Nature (London) **337**, 345–347 (1989).
[2] P. Fournier *et al.,* in *The Gap Symmetry and Fluctuations in High Temperature Superconductors,* edited by J. Bok *et al.,* NATO Advanced Study Institutes, Vol. 371 (Plenum, New York, 1998), p. 145.
[3] Y. Onose *et al.,* Phys. Rev. Lett. **82**, 5120 (1999).
[4] N. P. Armitage *et al.,* Phys. Rev. Lett. **86**, 1126 (2001).
[5] D. King *et al.,* Phys. Rev. Lett. **70**, 3159 (1993); R. O. Anderson *et al.,* Phys. Rev. Lett. **70**, 3163 (1993).
[6] A line of symmetrized data points was used immediately below and parallel to the zone diagonal as these points were missing from our initial data set.
[7] S. Massida, N. Hamada, J. Yu, and A. Freeman, Physica (Amsterdam) **157C**, 571–574 (1989).
[8] G. Kotliar and J. Liu, Phys. Rev. B **38**, 5142 (1988); H. Fukuyama, Prog. Theor. Phys. Suppl. **108**, 287 (1992); P. A. Lee and X. G. Wen, Phys. Rev. Lett. **76**, 503 (1996).
[9] D. Pines, Z. Phys. B **103**, 129 (1997); J. Schmalian, D. Pines, and B. Stojkovic, Phys. Rev. Lett. **80**, 3839 (1998); A. P. Kampf and J. R. Schrieffer, Phys. Rev. B **42**, 7967 (1990).
[10] K. Yamada *et al.,* J. Phys. Chem. Solids **60**, 1025 (1999).
[11] R. Hlubina and T. M. Rice, Phys. Rev. B **51**, 9253 (1995).
[12] S. Chakravarty *et al.,* Phys. Rev. B **63**, 094503 (2001).
[13] N. Furukawa, T. M. Rice, and M. Salmhofer, Phys. Rev. Lett. **81**, 3195 (1998); C. Honerkamp *et al.,* Phys. Rev. B **63**, 035109 (2001).
[14] D. S. Marshall *et al.,* Phys. Rev. Lett. **76**, 4841 (1996).